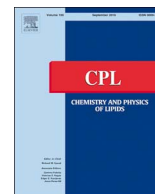




Contents lists available at ScienceDirect

Chemistry and Physics of Lipids

journal homepage: www.elsevier.com/locate/chemphyslip

Cobalt and nickel affect the fluidity of negatively-charged biomimetic membranes

Jenelle Umbsaar, Evan Kerek, Elmar J. Prenner*

Department of Biological Sciences, University of Calgary, Calgary, Alberta, T2N 1N4, Canada

ARTICLE INFO

Keywords:

Cobalt
Nickel
Liposomes
Laurdan
Membrane fluidity
Dynamic light scattering

ABSTRACT

Elevated levels of the essential trace metals cobalt and nickel are associated with a variety of toxic effects, which are not well-understood, and may involve interactions with the lipid membrane. Fluidity changes of biomimetic lipid membranes upon exposure to CoCl_2 and NiCl_2 were studied using the fluorescent probe Laurdan, which senses changes in environment polarity. Liposomes were prepared by extrusion in 20 mM HEPES + 100 mM NaCl at pH 7.4. Additionally, dynamic light scattering was used to monitor metal induced size changes of liposomes composed of: phosphatidic acid (PA), cardiolipin (CL), phosphatidylglycerol (PG), phosphatidylserine (PS), and phosphatidylcholine (PC), with saturated and unsaturated acyl chains. Micromolar concentrations of both metals significantly rigidify negatively-charged liposomes and generally increase the melting temperature. Saturated acyl chains showed stronger metal effects in PS and PG, while no clear acyl chain preference was observed in CL and PA systems. The strength of the effect appears to be influenced greatly by both the head group and acyl chain. The rigidifying effects of cobalt were almost always much larger than those of nickel. In addition, size changes and aggregation by both metals was detected in PS or PA liposomes at molar metal/lipid ratios as low as 1/10.

1. Introduction

The transition metals cobalt (Co) and nickel (Ni) are generally classified as essential trace elements, as Co is the coordinating metal in the structure of vitamin B_{12} (Barceloux, 1999a). The biological function of Ni in humans is unclear, but there are indications for a role in iron absorption and metabolism based on animal studies (Das et al., 2008; Denkhaus and Salnikow, 2002). The main route of uptake of both metals is through the diet, with estimated daily intakes of 11 μg of cobalt and 286 μg of nickel (Dabeka and McKenzie, 1995) while exposure to excess of either metal may cause cancer, lung and cardiovascular disease, and neurotoxicity (Barceloux, 1999a; Catalani et al., 2012; Denkhaus and Salnikow, 2002). The industrialization of modern society has brought about increased exposure to these metals, as they are both very common in the manufacture of many products such as appliances, jewelry, and utensils (Barceloux, 1999a,b). Besides industry, Co is also used in medicine as the major component of metal-on-metal hip implants (Paustenbach et al., 2014). Due to their increased

prevalence, potential consequences of cobalt and nickel exposure in the workplace and home must be considered.

Routes of exposure to both metals include ingestion, inhalation, and dermal absorption (Barceloux, 1999a,b). Gastrointestinal absorption generally occurs in the range of 5–20% for Co salts (Barceloux, 1999a), and 1–5% for Ni salts (Barceloux, 1999b), while the extent of absorption depends on and influences iron levels (Barceloux, 1999a; Denkhaus and Salnikow, 2002), likely due to uptake by a broad-specificity ion channel (Gunshin et al., 1997). Healthy blood concentrations of both Co and Ni are in the nanomolar range (Barceloux, 1999a,b). It has been suggested that blood concentrations of 5 μM Co are tolerable for the general population, while cardiomyopathy and neurotoxicity have been reported in the 12–14 μM range (Paustenbach et al., 2014). A case study on acute Ni poisoning via occupational exposure to contaminated water found blood concentrations of 0.2–23 μM resulting in a series of symptoms including nausea, shortness of breath and diarrhea (Sunderman et al., 1988) whereas others reported similar effects at a concentration of 50 μM (Webster et al., 1980). Therefore, it seems

Abbreviations: Co, cobalt; Ni, nickel; T_m , membrane phase transition temperature; GP, generalized polarization; DLS, dynamic light scattering; LUVs, large unilamellar vesicles; MLVs, multilamellar vesicles; POPC, 1-palmitoyl-2-oleoyl-*sn*-glycero-3-phosphocholine; DMPC, 1,2-dimyristoyl-*sn*-glycero-3-phosphocholine; POPE, 1-palmitoyl-2-oleoyl-*sn*-glycero-3-phosphoethanolamine; POPA, 1-palmitoyl-2-oleoyl-*sn*-glycero-3-phosphate; DMPA, 1,2-dimyristoyl-*sn*-glycero-3-phosphate; TOCL, 1',3'-bis[1,2-dioleoyl-*sn*-glycero-3-phospho]-*sn*-glycerol; TMCL, 1',3'-bis[1,2-dimyristoyl-*sn*-glycero-3-phospho]-*sn*-glycerol; POPG, 1-palmitoyl-2-oleoyl-*sn*-glycero-3-phospho-(1'-*rac*-glycerol); DMPG, 1,2-dimyristoyl-*sn*-glycero-3-phospho-(1'-*rac*-glycerol); POPS, (1-palmitoyl-2-oleoyl-*sn*-glycero-3-phospho)-*l*-serine; DMPS, 1,2-dimyristoyl-*sn*-glycero-3-phospho-*l*-serine

* Corresponding author.

E-mail address: eprenner@ucalgary.ca (E.J. Prenner).<https://doi.org/10.1016/j.chemphyslip.2017.11.016>Received 15 August 2017; Received in revised form 2 November 2017; Accepted 24 November 2017
0009-3084/ © 2017 Published by Elsevier Ireland Ltd.

pertinent to consider that toxic effects may be induced by Co or Ni ions in the micromolar range. The majority of both metals are excreted fairly rapidly, with Ni having a half-life of 20–60 h (Barceloux, 1999b), and Co of several days (Barceloux, 1999a); however, Co can accumulate in the kidney, pancreas, liver, heart and skeletal muscle for years (Barceloux, 1999b; Simonsen et al., 2012) while Ni, a known carcinogen, may accumulate in the lungs (Denkhaus and Salmikow, 2002).

The specific modes of toxicity of Co and Ni are not well-understood, as many biomolecular interactions, both direct and indirect, occur in the human body. In their divalent form, both metals bind to human serum albumin at three distinct sites, which influences metal transport and bioavailability (Sokołowska et al., 2009). The metals are primarily taken up into cells using calcium ion channels (Kasprzak, 2003; Simonsen et al., 2012). Both metals cause lipid peroxidation in the presence of iron, suggesting that they either stimulate iron through their redox capacity, or bind to lipids and promote radical propagation (Repetto et al., 2010). The occurrence of lipid peroxidation suggests metal localization and interaction with the membrane. The effects of toxic levels of metals on lipids are important, as the membrane functions as a crucial barrier towards the outside environment. As well, the membrane is involved in signaling and transport, and proper fluidity and permeability are essential for cellular function.

The interactions of metals with membranes strongly depend on metal speciation and the experimental conditions (Payliss et al., 2015). In this case, the metal-lipid interactions were studied under physiological conditions of 100 mM NaCl and pH 7.4. The VMINTEQ 3.1 program (Gustafsson, 2011), used to determine the metal speciation, predicted almost entirely divalent positively-charged species for Co and Ni under these conditions. Therefore, it is likely that they interact with negatively-charged lipids. Moreover, the affinity of the metals for buffers must be considered to avoid unspecific binding (Jahromi et al., 2010) and HEPES was found to be a suitable buffer because it did not exhibit appreciable binding for either metal (Sokołowska et al., 2009). To identify preferential lipid targets for both metals, Large Unilamellar Vesicles (LUVs) composed of different lipid classes were screened in terms of metal effects on membrane fluidity, which was assessed by using the fluorophore Laurdan. This solvent-sensitive probe exhibits a red shift of its emission maximum in a more polar environment and can also be used to determine metal effects on membrane phase transition temperature (T_m) and fluidity (Parasassi et al., 1998). This approach has been previously used to investigate the metal-induced fluidity changes of cadmium (Cd) (Kerek and Prenner, 2016) and mercury (Hg) (Kerek et al., 2017) for charged, neutral and zwitterionic membranes. In addition, metal effects on the size of the LUVs were investigated by Dynamic Light Scattering (DLS) since metal induced aggregation has been reported for various metals including calcium (Ca) (Düzgünes et al., 1981; Koter et al., 1978) and cadmium (Cd) (Kerek and Prenner, 2016). The results of the present study have indicated that negatively-charged lipids constitute binding targets of Co and Ni, as interaction caused membrane rigidification and liposome aggregation.

2. Materials and methods

2.1. Reagents

Lipid powders were purchased from Avanti Polar Lipids (Alabaster, AL), including: 1-palmitoyl-2-oleoyl-*sn*-glycero-3-phosphocholine (POPC), 1,2-dimyristoyl-*sn*-glycero-3-phosphocholine (DMPC), 1-palmitoyl-2-oleoyl-*sn*-glycero-3-phosphoethanolamine (POPE), 1-palmitoyl-2-oleoyl-*sn*-glycero-3-phosphate (POPA), 1,2-dimyristoyl-*sn*-glycero-3-phosphate (DMPA), 1',3'-bis[1,2-dioleoyl-*sn*-glycero-3-phospho]-*sn*-glycerol (TOCL), 1',3'-bis[1,2-dimyristoyl-*sn*-glycero-3-phospho]-*sn*-glycerol (TMCL), 1-palmitoyl-2-oleoyl-*sn*-glycero-3-phospho-(1'-*rac*-glycerol) (POPG), 1,2-dimyristoyl-*sn*-glycero-3-phospho-(1'-*rac*-glycerol) (DMPG), 1-palmitoyl-2-oleoyl-*sn*-glycero-3-phospho-L-serine (POPS), 1,2-dimyristoyl-*sn*-glycero-3-phospho-L-serine

(DMPS). 6-Dodecanoyl-2-Dimethylaminonaphthalene (Laurdan) was purchased from Molecular Probes (Eugene, OR). NiCl₂, HEPES (4-(2-hydroxyethyl)-1-piperazineethanesulfonic acid), and phosphate assay reagents (MgNO₃·6H₂O, Ascorbic acid, (NH₄)₆Mo₇O₂₄·4H₂O) were purchased from Sigma-Aldrich (Oakville, ON). CoCl₂ was purchased from Allied Chemical (Morristown, U.S.A.).

2.2. LUV preparation

Lipid films were prepared by co-dissolving lipid powders in 7:3 chloroform-methanol with Laurdan at a 1/275 Laurdan/lipid molar ratio, which provided sufficient signal without affecting the membrane properties (Kerek and Prenner, 2016; Pande et al., 2005). The solvent was evaporated under argon and subsequently dried overnight in a vacuum to remove solvent traces. Films were rehydrated above the membrane T_m and resuspended by sonication, vortexing, and freeze-thaw cycles in 20 mM HEPES, 100 mM NaCl buffer at pH 7.4. The LUVs were formed using an extruder (Avanti Polar Lipids, Alabaster, AL) with 100 nm diameter Whatman Nucleopore polycarbonate filters (Maidstone, UK). The samples were passed through the filter 30 times. Following extrusion, the phospholipid concentration was determined according to Ames (Ames, 1966).

2.3. Fluorescence measurements

Fluorescence measurements were performed on a Cary Eclipse fluorimeter (Agilent Technologies, Santa Clara, CA) by excitation at 340 nm, measuring emission at both 440 nm and 490 nm as an average of 4 measurements with 5 nm excitation and emission bandpasses. 0.3 mM LUVs were combined in small volume quartz cuvettes (Starna Scientific Ltd, Atascadero, CA) with 15–1200 μ M CoCl₂ or NiCl₂. Metal was added to the samples at room temperature and allowed to incubate for 10 min prior to experiments. Temperature was controlled within 0.1 °C by a Cary water bath temperature controller (Agilent Technologies, Santa Clara, CA). Measurements were performed between 10 and 60 °C; the detailed ranges varied for the individual lipids depending on the T_m . Samples were equilibrated for at least 1 min/1 °C change. T_m 's were determined by fitting the GP versus temperature curve to the Boltzmann function in OriginPro 8 software (Origin Lab Corporation, 2008), in which A_1 and A_2 are the initial and final x (temperature) values, x_0 is the inflection point, representing the T_m , and dx is a time constant.

$$Y = A_2 + \frac{A_1 - A_2}{1 + \exp\left(\frac{x - x_0}{dx}\right)} \quad (1)$$

2.4. Dynamic light scattering (DLS)

Size measurements were performed at 25 °C on a Zetasizer Nano-ZS (Malvern, Worcestershire, UK) in which triplicate measurements of the mean radius were averaged. 0.3 mM LUVs were incubated for 15 min with various concentrations of CoCl₂ or NiCl₂.

2.5. Statistical analysis

Significant differences were assessed by performing *t*-tests assuming unequal variances at the 95% confidence level. Figures show error bars representing \pm standard deviation comparing raw GP or T_m values. Asterisks in figures represent levels of significance: $p < 0.05$ (*), $p < 0.01$ (**), $p < 0.001$ (***), $p < 0.0001$ (****).

Download English Version:

<https://daneshyari.com/en/article/7692172>

Download Persian Version:

<https://daneshyari.com/article/7692172>

[Daneshyari.com](https://daneshyari.com)